Variational Monte Carlo study for the insulating mechanism of Sr_2IrO_4: from the viewpoint of energy gain

Hiroshi Watanabe[1,2,3], **Tomonori Shirakawa**[1,2,3] **and Seiji Yunoki**[1,2,3]

[1]Computational Condensed Matter Physics Laboratory, RIKEN ASI, Saitama 351-0198, Japan
[2]CREST, Japan Science and Technology Agency (JST), Saitama 332-0012, Japan
[3]Computational Materials Science Research Team, RIKEN AICS, Kobe, Hyogo 650-0047, Japan

E-mail: `h-watanabe@riken.jp`

Abstract. To examine the insulating mechanism of a novel $5d$-electron system Sr_2IrO_4, we study the ground state properties of a three-orbital Hubbard model using a variational Monte Carlo method. We find that the insulating state in the ground state phase diagram shows crossover behavior from a weakly-correlated to a strongly-correlated antiferromagnetic state. This crossover is characterized by the different mechanisms of the insulating state, i.e., changing from an interaction-energy driven insulator to a band-energy driven insulator with increasing the interaction. We discuss that Sr_2IrO_4 is located around this crossover region and displays an anomalous behavior.

1. Introduction

Recently, a $5d$ transition metal oxide Sr_2IrO_4 [1] has attracted much attention. In this material, three t_{2g} orbitals of Ir atoms are hybridized with each other by the large spin-orbit coupling (SOC) of $5d$ electrons, and nominally five $5d$ electrons occupy these orbitals. Because of this quantum entanglement of spin and orbital degrees of freedom, an effective total angular momentum $J_{\rm eff}=|\boldsymbol{L}-\boldsymbol{S}| = 1/2$ state is stable locally at each Ir atom. As a result, many interesting properties are experimentally observed, which include a novel $J_{\rm eff} = 1/2$ insulating state [2, 3, 4, 5]. The origin of this insulating state is still under debate: Although the Mott-Hubbard type mechanism (i.e., a strongly-correlated insulator) is originally proposed for Sr_2IrO_4 [2, 3], there are several reports suggesting the Slater type mechanism (i.e., a weakly-correlated insulator) [6, 7, 8]. It should be noted, however, that experimentally the temperature dependence of the resistivity is found insulating and no significant change is observed at the Néel temperature [9], strongly suggesting that Sr_2IrO_4 is a Mott-Hubbard type insulator. In this paper, we study the ground state properties of a three-orbital Hubbard model using a variational Monte Carlo (VMC) method and examine the insulating mechanism of Sr_2IrO_4 from the viewpoint of energy gain.

2. Model and method

We consider a three-orbital Hubbard model on a two-dimensional square lattice defined by the following Hamiltonian $H = H_{\rm kin} + H_{\rm SO} + H_{\rm I}$, where $H_{\rm kin} = \sum_{\boldsymbol{k}\alpha\sigma} \varepsilon_\alpha(\boldsymbol{k}) c^\dagger_{\boldsymbol{k}\alpha\sigma} c_{\boldsymbol{k}\alpha\sigma}$ is the kinetic

term, $H_{\mathrm{SO}} = \lambda \sum_i \boldsymbol{L}_i \cdot \boldsymbol{S}_i$ is the SOC term with a coupling constant λ, and

$$
\begin{aligned}
H_{\mathrm{I}} = &\, U \sum_{i,\alpha} n_{i\alpha\uparrow} n_{i\alpha\downarrow}, \\
&+ \sum_{i,\alpha<\beta,\sigma} \left[U' n_{i\alpha\sigma} n_{i\beta\bar{\sigma}} + (U'-J) n_{i\alpha\sigma} n_{i\beta\sigma} \right] \\
&+ J \sum_{i,\alpha<\beta} \left(c^{\dagger}_{i\alpha\uparrow} c^{\dagger}_{i\beta\downarrow} c_{i\alpha\downarrow} c_{i\beta\uparrow} + c^{\dagger}_{i\alpha\uparrow} c^{\dagger}_{i\alpha\downarrow} c_{i\beta\downarrow} c_{i\beta\uparrow} + \mathrm{H.c.} \right)
\end{aligned}
\tag{1}
$$

is the Coulomb interactions including intraorbital (U), interorbital (U'), and spin-flip and pair-hopping (J) interactions. Here, $c^{\dagger}_{i\alpha\sigma}$ is a creation operator of electron at site i, spin $\sigma(=\uparrow,\downarrow)$, and orbital $\alpha(= yz, zx, xy)$ corresponding three t_{2g} orbitals.

The kinetic and SOC terms can be represented ($H_0 = H_{\mathrm{kin}} + H_{\mathrm{SO}}$) in the matrix form,

$$
\begin{aligned}
H_0(t_i, \mu_3, \lambda) &= \sum_{\boldsymbol{k}\sigma} \left(c^{\dagger}_{\boldsymbol{k}yz\sigma}, c^{\dagger}_{\boldsymbol{k}zx\sigma}, c^{\dagger}_{\boldsymbol{k}xy\bar{\sigma}} \right)
\begin{pmatrix}
\varepsilon_{yz}(\boldsymbol{k}) & \mathrm{i}\sigma\lambda/2 & -\sigma\lambda/2 \\
-\mathrm{i}\sigma\lambda/2 & \varepsilon_{zx}(\boldsymbol{k}) & \mathrm{i}\lambda/2 \\
-\sigma\lambda/2 & -\mathrm{i}\lambda/2 & \varepsilon_{xy}(\boldsymbol{k})
\end{pmatrix}
\begin{pmatrix}
c_{\boldsymbol{k}yz\sigma} \\
c_{\boldsymbol{k}zx\sigma} \\
c_{\boldsymbol{k}xy\bar{\sigma}}
\end{pmatrix} \\
&= \sum_{\boldsymbol{k}ms} E_m(\boldsymbol{k}) a^{\dagger}_{\boldsymbol{k}ms} a_{\boldsymbol{k}ms},
\end{aligned}
\tag{2}
$$

where $c^{\dagger}_{\boldsymbol{k}\alpha\sigma}$ is the Fourier transformation of $c^{\dagger}_{i\alpha\sigma}$. Notice that the SOC mixes the three orbitals and up and down spins, and the new quasiparticles, obtained by diagonalizing H_0, are characterized by the band index m and pseudospin s with a creation operator $a^{\dagger}_{\boldsymbol{k}ms}$. In the atomic limit ($\varepsilon_{yz}(\boldsymbol{k}) = \varepsilon_{zx}(\boldsymbol{k}) = \varepsilon_{xy}(\boldsymbol{k}) = 0$), the sixfold degenerate states are split into doubly degenerate $J_{\mathrm{eff}} = 1/2$ states and fourfold degenerate $J_{\mathrm{eff}} = 3/2$ states [2].

First, the non-interacting tight-binding energy band is constructed so as to reproduce the result of LDA+SO (spin-orbit) calculation [2] for $\mathrm{Sr_2IrO_4}$. The energy dispersion for three t_{2g} orbitals are defined as $\varepsilon_{yz}(\boldsymbol{k}) = -2t_5 \cos k_x - 2t_4 \cos k_y$, $\varepsilon_{zx}(\boldsymbol{k}) = -2t_4 \cos k_x - 2t_5 \cos k_y$, and $\varepsilon_{xy}(\boldsymbol{k}) = -2t_1(\cos k_x + \cos k_y) - 4t_2 \cos k_x \cos k_y - 2t_3(\cos 2k_x + \cos 2k_y) + \mu_3$ [4]. Here, we choose a set of parameters $(t_1, t_2, t_3, t_4, t_5, \mu_3, \lambda)$=(0.36, 0.18, 0.09, 0.37, 0.06, -0.36, 0.50) eV. In the following, we use t_1 as an energy unit.

Next, we introduce the the following Gutzwiller-Jastrow type trial wave function: $|\Psi\rangle = P_{\mathrm{J_c}} P_{\mathrm{G}} |\Phi\rangle$. $|\Phi\rangle$ is the one-body part of the wave function, constructed from the ground state of N_e number of electrons for $\bar{H}_0(\tilde{t}_i, \tilde{\mu}_3, \tilde{\lambda}_{\alpha\beta})$, where $\tilde{t}_i$, $\tilde{\mu}_3$, and $\tilde{\lambda}_{\alpha\beta}$ are variational parameters. As an effect of the many-body Coulomb interaction, the "effective" coupling constant of the SOC has orbital dependence: $\lambda \rightarrow \tilde{\lambda}_{\alpha\beta}$. To consider magnetically ordered states, a term with magnetic order parameters is added to $\bar{H}_0$. Here, we consider the commensurate antiferromagnetic (AF) state with an ordering vector $\boldsymbol{Q} = (\pi, \pi)$. Two states considered are i) an out-of-plane AF order (along z axis) and ii) an in-plane AF order (along x axis), described by $\sum_{i,m} M^z_m \mathrm{e}^{\mathrm{i}\boldsymbol{Q}\cdot\boldsymbol{r}_i}(a^{\dagger}_{im\uparrow} a_{im\uparrow} - a^{\dagger}_{im\downarrow} a_{im\downarrow})$ and $\sum_{i,m} M^x_m \mathrm{e}^{\mathrm{i}\boldsymbol{Q}\cdot\boldsymbol{r}_i}(a^{\dagger}_{im\uparrow} a_{im\downarrow} + a^{\dagger}_{im\downarrow} a_{im\uparrow})$, respectively. These two AF states have different energies in general since the rotational symmetry in a spin space is broken due to the SOC and the Hund's coupling J. However, here we consider only the case of $J = 0$ and thus they are energetically degenerated [4].

For the trial wave function of superconducting states, we consider a BCS-type one in a pseudospin representation,

$$
|\Phi\rangle \propto \left(\sum_{\boldsymbol{k}mn} f_{\boldsymbol{k}mn} a^{\dagger}_{\boldsymbol{k}m\uparrow} a^{\dagger}_{\boldsymbol{k}n\downarrow} \right)^{N_e/2} |0\rangle .
\tag{3}
$$
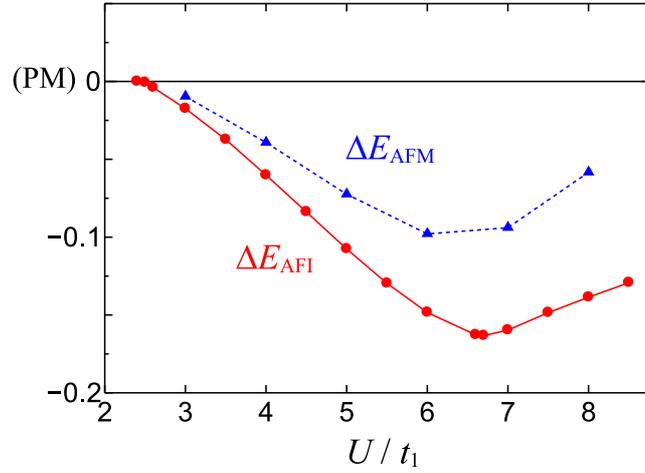
Figure 1. (color online) The condensation energy $\Delta E(U)$ defined as the energy difference between the AF and the paramagnetic states [see (4)]. ΔE_{AFI} and ΔE_{AFM} denote the condensation energies of AF insulating and metallic states. Here, $n = 5, \lambda/t_1 = 1.4$, and $J/U = 0$ are used. Statistical errors are within the width of the symbols.

Here, $f_{\boldsymbol{k}mn}$ is obtained by diagonalizing BCS-type Hamiltonian with three energy bands (6×6 matrix) and the explicit form is given in [10].

$P_{\mathrm{G}} = \prod_{i,\gamma} [1 - (1 - g_\gamma) |\gamma\rangle \langle\gamma|_i]$ in $|\Psi\rangle$ is a Gutzwiller factor extended to the three-orbital system [4]. i represents a site index and γ runs over all possible electron configurations at each site. For the three-orbital system, there are $4^3 = 64$ electron configurations, namely, $|0\rangle = |0\ 0\ 0\rangle$, $|1\rangle = |0\ 0\ \uparrow\rangle$, $\cdots$, $|63\rangle = |\uparrow\downarrow\ \uparrow\downarrow\ \uparrow\downarrow\rangle$. g_γ is a weight of each electron configuration, and it takes the value from 0 to 1, controlling the local electron correlations. In this study, we classify the possible 64 patterns into 12 groups by the Coulomb interaction energy, and g_γ's in the same group are set to be the same.

$P_{\mathrm{J_c}} = \exp\left[-\sum_{i \neq j} v_{ij} n_i n_j\right]$ in $|\Psi\rangle$ is a charge Jastrow factor that controls the long-range charge correlations. Here, we assume that v_{ij} depends only on the distances, $v_{ij} = v(|\boldsymbol{r}_i - \boldsymbol{r}_j|)$ and consider all independent v_{ij}. For example, there are 41 independent v_{ij}'s for 16×16, taking into account up to the 41st-neighbor correlation.

Using the trial wave functions described above, we optimize the variational parameters to minimize the variational energy using the stochastic reconfiguration method [11]. Comparing the variational energy for paramagnetic, AF, and superconducting states, we determine the ground state phase diagram. For large size calculations, parallel computing is indispensable. The VMC method can be efficiently parallelized by distributing the independent Monte Carlo samplings to different processors. We parallelize the simulations using 32–128 processors and the total number of Monte Carlo samples taken is about 10^5–10^6, for example, $10,000 \times 64$ samples using 64 processors with $10,000$ independent samples for each processor.

3. Results
We study the ground state properties of the three-orbital Hubbard model on a 16×16 square lattice with electron density $n = 5$. In this paper, we consider only $J = 0$ and we impose the condition $U = U' + 2J$ [12], thus $U = U'$.
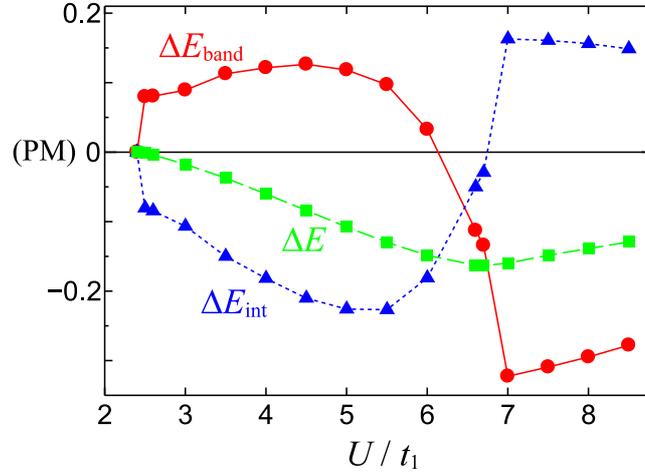
Figure 2. (color online) The condensation energy $\Delta E(U) = \Delta E_{\text{band}}(U) + \Delta E_{\text{int}}(U)$ defined as the energy difference between the AF insulating and the paramagnetic states. $\Delta E_{\text{band}}(U)$ and $\Delta E_{\text{int}}(U)$ are two separate contribution from the band energy and the interaction energy, respectively. Here, $n = 5, \lambda/t_1 = 1.4$, and $J/U = 0$ are used. Statistical errors are within the width of the symbols.

First, we calculate the condensation energy of the AF state, which is defined by

$$\Delta E(U) = E_{\text{AF}} - E_{\text{PM}}, \tag{4}$$

with varying U. Here, E_{AF} (E_{PM}) is the optimized variational energy of the AF (paramagnetic metallic) state for a given value of U. The critical U_{AF} for the AF order is where $\Delta E(U = U_{\text{AF}}) = 0$. We find that with increasing U, the AF transition occurs at around $U_{\text{AF}}/t_1 \sim 2.5$. Furthermore, we find that a metal-insulator transition occurs simultaneously and the system becomes an AF insulator. Namely, an AF metallic state has always larger variational energy than the AF insulating state, as shown in figure 1, and thus it is unstable. We also calculate the variational energies of the possible superconducting states and find that the one with $d_{x^2-y^2}$ symmetry has the smallest variational energy. However, its variational energy is always much larger than the AF insulating state and therefore the superconducting state is not the ground state for this electron density.

Next, to study the character of the AF insulating state, we examine the origin of this negative condensation energy $\Delta E(U)$ in the AF insulating state. Let us divide $\Delta E(U)$ into two parts,

$$\Delta E(U) = \Delta E_{\text{kin}} + \Delta E_{\text{SO}} + \Delta E_U + \Delta E_{U'} + \Delta E_J + \Delta E_{J'}$$
$$= \Delta E_{\text{band}}(U) + \Delta E_{\text{int}}(U), \tag{5}$$

where $\Delta E_{\text{band}}(U) = \Delta E_{\text{kin}} + \Delta E_{\text{SO}}$ is the contribution from the band (i.e., kinetic and SOC) energy and $\Delta E_{\text{int}}(U) = \Delta E_U + \Delta E_{U'} + \Delta E_J + \Delta E_{J'}$ is the contribution from the interaction (i.e., Coulomb) energy. Figure 2 shows the U dependences of $\Delta E(U)$, $\Delta E_{\text{band}}(U)$, and $\Delta E_{\text{int}}(U)$. For small U, the energy gain of the AF insulating state is due to the interaction energy, i.e., $\Delta E_{\text{int}}(U) < 0$ but $\Delta E_{\text{band}}(U) > 0$, indicating that this AF insulator is interaction-energy driven. Instead, for large U, the AF insulating state is stabilized due to the band energy gain, i.e., $\Delta E_{\text{band}}(U) < 0$ but $\Delta E_{\text{int}}(U) > 0$, strongly suggesting that this AF insulator is band-energy driven. It is also clear in figure 2 that there is a crossover region $U_{\text{co}}/t_1 \sim 6.5$ where
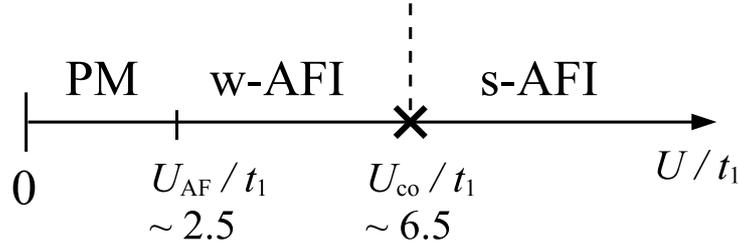
Figure 3. The ground state phase diagram for $n = 5$, $\lambda/t_1 = 1.4$, and $J/U = 0$, obtained from figure 2. PM, w-AFI, and s-AFI denote a paramagnetic metallic, a weakly-correlated AF insulating, and a strongly-correlated AF insulating states, respectively.

$\Delta E_{\text{band}}(U)$ and $\Delta E_{\text{int}}(U)$ are both negative and intersect. Note that this crossover is not a phase transition because both insulating states are described by the same AF insulating wave function. However, this crossover should be considered to be a boundary separating a weakly-correlated and a strongly-correlated regions. The ground state phase diagram is summarized in figure 3. The same kind of crossover for a AF and a superconducting states is also discussed in a single-orbital Hubbard model [13, 14, 15, 16] and the results are consistent with ours for the three-orbital Hubbard model.

There are several reports estimating the values of the Coulomb interactions for Ir oxides [7, 17, 18]. According to the constrained RPA calculation [7], the value of U is estimated as large as ~ 2.3 eV, corresponding to $U/t_1 \sim 6.5$ in our model. This value is very close to $U_{\text{co}}/t_1 \sim 6.5$ as seen in figure 3. We also found that U_{co} depends on the values of λ/t_1 and J/U (a smaller λ/t_1 or a larger J/U increases U_{co}), however, these effects are only quantitative and overall behaviors of $\Delta E_{\text{band}}(U)$, $\Delta E_{\text{int}}(U)$, and $\Delta E(U)$ are unchanged. Our result strongly indicates that Sr_2IrO_4 should be located at around the crossover region separating the Slater type and the Mott-Hubbard type insulators. Therefore, it is very natural to expect that Sr_2IrO_4 can exhibit dual characteristics of weakly-correlated and strongly-correlated natures.

4. Summary
In this paper, using the variational Monte Carlo method, we have studied the ground state properties of the three-orbital Hubbard model for Sr_2IrO_4. We have found that the insulating state in the ground state phase diagram shows a crossover from the weakly-correlated AF insulating state to the strongly-correlated AF insulating state, i.e., from the interaction-energy driven to the band-energy driven AF insulating state. Our result suggests that Sr_2IrO_4 is located at around this crossover region and can display an anomalous behavior.

References
[1] Randall J J *et al.* 1957 *J. Am. Chem. Soc.* **79** 266
[2] Kim B J *et al.* 2008 *Phys. Rev. Lett.* **101** 076402
[3] Kim B J, Ohsumi H, Komesu T, Sakai S, Morita T, Takagi H, Arima T 2009 *Science* **323** 1329

[4] Watanabe H, Shirakawa T and Yunoki S 2010 *Phys. Rev. Lett.* **105** 216410

[5] Shirakawa T, Watanabe H and Yunoki S 2011 *J. Phys. Soc. Jpn.* **80** SB010

[6] Kini N S, Strydom A M, Jeevan H S, Geibel C and Ramakrishnan S 2006 *J. Phys.: Condens. Matter* **18** 8205

[7] Arita R, Kuneš J, Kozhevnikov A V, Eguiluz A G and Imada M 2012 *Phys. Rev. Lett.* **108** 086403

[8] Hsieh D, Mahmood F, Torchinsky D H, Cao G and Gedik N 2012 *Phys. Rev. B* **86** 035128

[9] Chikara S, Korneta O, Crummett W P, DeLong L E, Schlottmann P and Cao G 2009 *Phys. Rev. B* **80** 140407(R)

[10] Watanabe H, Shirakawa T and Yunoki S 2013 *Phys. Rev. Lett.* **110** 027002

[11] Sorella S 2001 *Phys. Rev. B* **64** 024512; Casula M and Sorella S 2003 *J. Chem. Phys.* **119** 6500; Casula M, Attaccalite C and Sorella S 2004 *J. Chem. Phys.* **121** 7110; Yunoki S and Sorella S 2006 *Phys. Rev. B* **74** 014408; Sorella S, Casula M and Rocca D, *J. Chem. Phys.* **127** 014105

[12] Kanamori J, 1963 *Prog. Theor. Phys.* **30** 275

[13] Yokoyama H, Tanaka Y, Ogata M and Tsuchiura H 2004 *J. Phys. Soc. Jpn.* **73** 1119

[14] Maier Th A, Jarrell M, Macridin A and Slezak C 2004 *Phys. Rev. Lett.* **92** 027005

[15] Yanase Y and Ogata M 2005 *J. Phys. Soc. Jpn.* **74** 1534

[16] Yokoyama H, Ogata M, Tanaka Y, Kobayashi K and Tsuchiura H 2013 *J. Phys. Soc. Jpn.* **82** 014707

[17] Martins C, Aichhorn M, Vaugier L and Biermann S 2011 *Phys. Rev. Lett.* **107** 266404

[18] Comin R *et al.* 2012 *Phys. Rev. Lett.* **109** 266406; Kim B H, Khaliullin G and Min B I 2012 *Phys. Rev. Lett.* **109** 167205